A multiswitchable poly(terthiophene) bearing a spiropyran functionality: understanding photo and electrochemical control.

Klaudia Wagner,[†] Robert Byrne,[‡] Michele Zanoni,[‡] Sanjeev Gambhir,[†] Lynn Dennany,[†] Robert Breukers,[†] Michael Higgins,[†] Pawel Wagner,[†] Dermot Diamond,[‡] Gordon G. Wallace[†] and David L. Officer[†]*

ARC Centre of Excellence for Electromaterials Science and Intelligent Polymer Research Institute, University of Wollongong, AIIM Facility, Innovation Campus, Wollongong, NSW 2519, Australia and National Centre for Sensor Research, Dublin City University, Collins Avenue, Glasnevin, Dublin, Ireland 9

*To whom correspondence should be addressed. E-mail: davido@uow.edu.au

[†] ARC Centre of Excellence for Electromaterials Science and Intelligent Polymer Research Institute, University of Wollongong, AIIM Facility, Innovation Campus, Wollongong, NSW 2519, Australia

[‡] National Centre for Sensor Research, Dublin City University, Collins Avenue, Glasnevin, Dublin, Ireland 9

ABSTRACT

An electroactive nitrospiropyran-substituted polyterthiophene, 2-(3,3′′-dimethylindoline-6′-nitrobenzospiropyranyl)ethyl 4,4′′-didecyloxy-2,2′:5′,2′′-terthiophene-3′-acetate, has been synthesized for the first time. The spiropyran, incorporated into the polymer backbone by covalent attachment to the alkoxyterthiophene monomer units, leads to multiple coloured states as a result of both electrochemical isomerization of the spiropyran moiety to merocyanine forms as well as electrochemical oxidation of the polyterthiophene backbone and the merocyanine substituents. While electrochemical polymerization of the terthiophene monomer could occurs without the apparent oxidation of the spiropyran, the subsequent electrochemistry is complex and clearly involves this substituent. In order to understand this complex behaviour, the first detailed electrochemical study of the oxidation of the precursor spiropyran, 1-(2-hydroxyethyl)-3,3-dimethylindoline-6'-nitrobenzospiropyran, was undertaken, showing that, in solution, an irreversible electrochemical oxidation of the spiropyran occurs leading to reversible redox behaviour of at least two merocyanine isomers. With these insights, an extensive electrochemical and spectroelectrochemical study of the nitrospiropyran-substituted polyterthiophene films reveals an initial irreversible electrochemical oxidative ring opening of the spiropyran to oxidized merocyanine. Subsequent reduction and cyclic voltammetry of the resulting nitromerocyanine-substituted polyterthiophene film gives rise to the formation of both merocyanine π-dimers or oligomers and π-radical cation dimers, between polymer chains. Although merocyanine formation is not electrochemically reversible, the spiropyran can be photochemically regenerated, at least in part, through irradiation with visible light. SEM and AFM images support the conclusion that the bulky spiropyran substituent is electrochemically isomerizes to the planar merocyanine moiety affording a smoother polymer film. The conductivity of the freestanding polymer film was found to be 0.4 S cm^{-1}.

1. Introduction

The immobilization of light–responsive molecules on electroactive surfaces provides an exciting opportunity for the development of smart materials and devices.[1] Spiropyrans, reported for the first time by Fischer and Hirshberg,[2] are one of the most widely studied classes of photoswitchable compounds. Irradiation of spiropyrans (**SP**, Figure 1) with near-UV light[3] or electro-oxidation[4] induces heterolytic cleavage of the spiro carbon-oxygen bond to produce ring-opened structures (**MC**, Figure 1), represented as two resonance forms, one merocyanine-like and the other quinoidal.

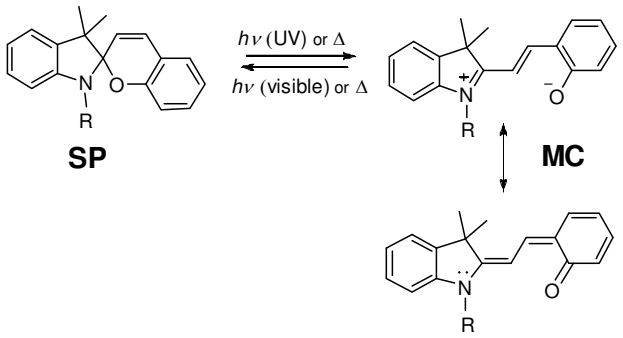

Figure 1. Benzospiropyran (**SP**, left) and its stimuli induced Zwitterionic and quinoidal isomers contribute to the open form (**MC**, right).

The intense absorption in the visible region of the open form **MC** has led to the advance study of spiropyrans in photochromic,[5] molecular optoelectronic[6] optobioelectronic fields,[7] and chemical sensing.[8]

The exploitation of such light-responsive molecules in devices typically requires immobilization on a surface through an appended functionality that does not interfere with the light switching behaviour. This has been achieved for photoswitchable molecules by formation of self-assembled monolayers (SAMs)[9] and bilayers[10] and incorporation into polymer films[11,12] and beads.[8] While the required structure for monolayer and bilayer formation does not usually affect the function of the photomolecules, one of the challenges in using polymers is that the monomer used to synthesis the polymer, and the polymerization process itself, must be compatible with the photo/electroactive

switching units. In addition, the incorporation of the photoresponsive functionality must not affect the polymerization of the monomer. Wesenhagen et al. recently reported the incorporation of photo/electrochromic dithienylcyclopentene moiety into a polymer by oxidative electropolymerization of a methoxystyryl monomer attached to the photoactive unit.[13] The electroactive polymer was formed as only a thin film, the thickness of several monolayers as the result of limited conductivity.

The photoswitchable moiety can be appended to the polymer backbone or incorporated into it with quite different effects. In the latter case, the incorporated photoswitchable unit can affect the nature of the polymer backbone. Hugel and co-workers have demonstrated that incorporation of azobenzene units into the backbone of the polymer chain modifies the modulus of elasticity of the polymer.[14] The nature of the polymer backbone can also influence kinetics of open/closed ring isomerization of the photoactive units, affect the stability or even lead to enhancement of photo degradation.[15]

While the introduction of photoswitchable molecules into polymers has proved valuable, the use of conducting polymers opens up a new avenue for electrochemical control of these multifunctional materials. In this regard, poly(thiophene) derivatives are of particular interest due to their stability and relative ease of synthesis and functionalization[16] and they have been applied in a broad range of devices, from simple solar cells[17] to complex electroluminescent devices.[18] This exciting potential of combining photoswitchability and electroactivity together was first recognized by Areephong et al. who reported the ability to control the electropolymerizability of an oligothiophene by the introduction of a photoswitchable dithienylethene unit into the monomer.[19] Most recently, the first spiropyran-functionalized polythiophene was obtained by chemical copolymerization of a thiophene monomer with covalently attached spiropyran and 3-hexylthiophene.[20] In this work, it was demonstrated that both the fluorescence of this photoswitchable conductive copolymer and its interactions with cyanide ions could be controlled through **SP** to **MC** photoconversion. However, the real benefit of combining the photoactivity and electrochemical activity of these materials was not explored.

The introduction of large functionalities onto a polythiophene can have a significant steric effect on the polymer backbone, adversely affecting the optical and electronic properties of the polymer as well

as the polymer processibility. The use of 4, 4''-dialkoxy-3-substituted terthiophenes as a precursor for developing novel substituted poly(thiophene)s provides reduced steric interactions between polymer backbone and substituent, allows better control of polymer regiochemistry, and the alkoxy side chains activate the monomer for polymerization and ensure better polymer processability.[21,22] We have been exploring successfully the polymerization of functionalized dialkoxyterthiophene monomers in order to avoid these problems.[22,23] Incorporation of the spiropyran moiety into a dialkoxyterthiophene monomer appeared to provide a good opportunity to investigate the potential for electrochemical control of photoresponsive functionality in a conducting polymer system. In this paper, we report the synthesis and properties of spiropyran-functionalized poly(terthiophene)s. The spiropyran unit is covalently linked to the monomer, which is electropolymerized. The resulting film is electroactive and shows multiswitchable behavior. In this exciting new material, we have electrochemical control of both the polymer redox and photochemical properties, as well as the ability to convert the **SP** to **MC** form with potential and light. To the best of our knowledge, this is the first report of the synthesis and electrochemical control of electropolymerized conductive polymer film bearing a spiropyran functionality.

2. Experimental Section

Experimental details are given in the Supporting Information.

3. Results and Discussion.

3.1. Synthesis of monomer. The dialkoxyterthiophene acetic acid **TThAA** was chosen in this study as the terthiophene monomer to functionalize with the **SP** group since mild chemistry can be used to form reasonably stable ester linkages with a readily available hydroxyl-substituted spiropyran, such as N-hydroxyethylnitrobenzospiropyran **SP1** (Scheme 1). Spiropyran-substituted terthiophene monomer **TThSP1** was readily prepared from the acetic acid **TThAA** (Scheme 1). The precursor methyl acetate

TThMA was synthesised as previously described[24] and hydrolysed to give **TThAA** in quantitative yield. Base catalysed condensation of **SP1** with **TThAA** afforded **TThSP1** in 77% yield.

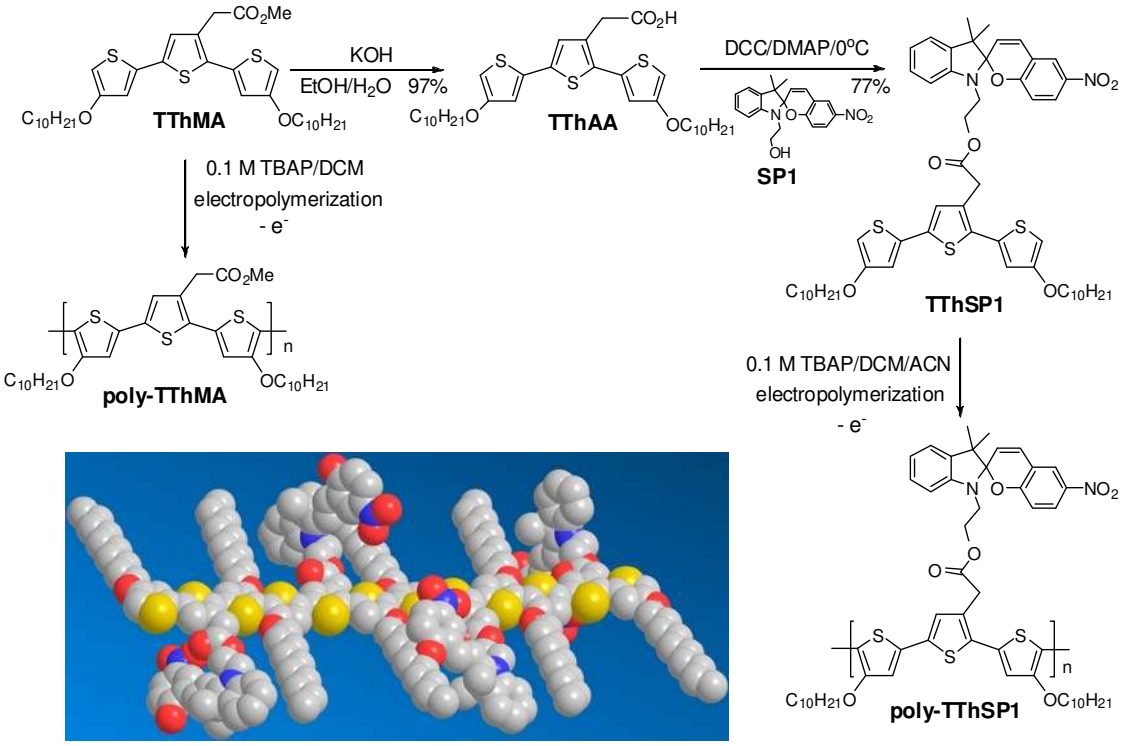

Scheme 1. Synthesis and polymerization of **TThSP1**. The inset shows a computer generated model of a short length of the ring-opened merocyanin polymer, **poly-TThMC1**.

The structures of the three substituted terthiophenes are fully consistent their spectroscopic data. The ^{1}H NMR terthiophene signals are as expected unperturbed by the change in ester functionality with NMR spectral characteristics of **TThSP1** simply being a superposition of the **TTh** and **SP** components.

As expected for nitrospiropyran derivatives, the UV-vis absorption spectrum of **TThSP1** (Figure 2, black line) shows bands in the ultraviolet (not shown) due to the **SP1** substituent. In the visible, the terthiophene absorbance dominates the spectrum at 350 nm, with no absorption due to the merocyanine isomer above 500 nm. Irradiation of a dichloromethane solution of **TThSP1** with UV light leads to the formation of **TThMC1** (Figure 2, violet line), as evidenced by the peak at 564 nm. This is analogous to the photochemical behaviour of **SP1** that gives the characteristic peak for a merocyanine at 560 nm

(**MC1**, Figure 2, red line). However, an additional band at 446 nm is also observed in the **MC1** spectrum. The origin of this peak has been explained by McCoy et al. who reported that nitro-spiropyran derivatives in dichloromethane isomerize to merocyanines and rapidly form H-aggregates, that exhibit a band at 446 nm.[25]

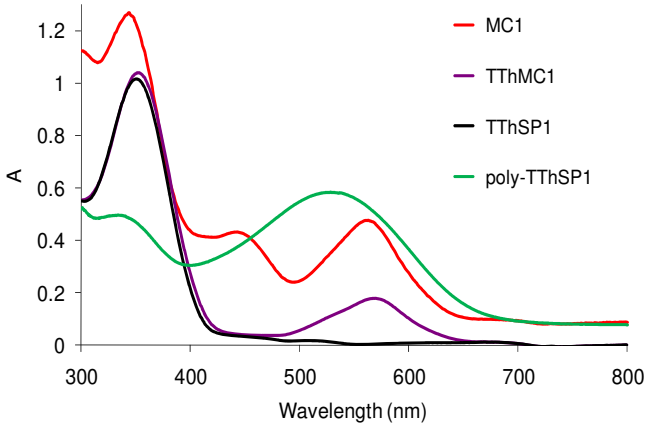

Figure 2. UV-vis spectra of: **MC1** after irradiation of **SP1** with 254 nm UV light (red line), monomer **TThSP1** at equilibrium (black line) and when irradiated with 254 nm UV light (violet line), and reduced **poly-TThSP1**. The concentration of **MC1** and **TThSP1** are 1 x 10^{-4} M in dichloromethane.

It seems therefore, that the terthiophene moiety does not affect the photochromic properties of the spiropyran substituent but does inhibit formation of aggregates.

3.2. Electrochemistry and spectroelectrochemistry of SP1. Our initial investigations into the electrochemical polymerization of **TThSP1** revealed that the resulting polymer had a more complex electrochemical behavior than expected from a substituted poly(thiophene). Since this behaviour clearly arose from the presence of spiropyran, and there appeared to be a limited knowledge of the electrochemistry of spiropyrans generally, we undertook an electrochemical study of **SP1**, which had not been investigated before.

The electrochemistry of analogues of **SP1** have been reported previously.[26-28] Zhi et al. discuss electrochemistry and spectroelectrochemistry of N-methylnitrobenzospiropyran, specifically investigating the reduction behaviour of the molecule but providing little information about the

oxidation of the spiropyran.[27] We do not observe the same electrooxidation characteristics as Zhi and co-workers. Our results are similar to Campredon et al.[26] who investigated the electrochemical behaviour of naphthalene analogues of **SP1**, although their report includes only a first scan of oxidation voltammograms and a brief comment regarding the instability and possible degradation of the formed radical cation. More recently, Jukes and co-workers[28] reported the electrochemistry and spectroelectrochemistry of 1,3,3-trimethylindolino-6'-nitrobenzopyrylospiran and, while they report oxidation voltammograms similar to ours, their focus is largely on the reduction influence on the oxidation.

On the first, positive scan on the **SP1** voltammogram (Figure 3a), one irreversible oxidation peak at the potential 0.77 V is observed, with broad, overlapping reduction waves on the reverse scan. It has been proposed that this first oxidation of spiro compounds is a one-electron oxidation at the indoline nitrogen.[4] Since the oxidation is irreversible, a new species must be formed from the oxidized spiropyran. Visual inspection of the solution at the working electrode surface (Figure 3e) during oxidation, shows the presence of an orange-red colour, similar to that observed by Preigh et al. during electrochemical oxidation of an hydroxyspiropyran and attributed to oxidized merocyanin.[4]

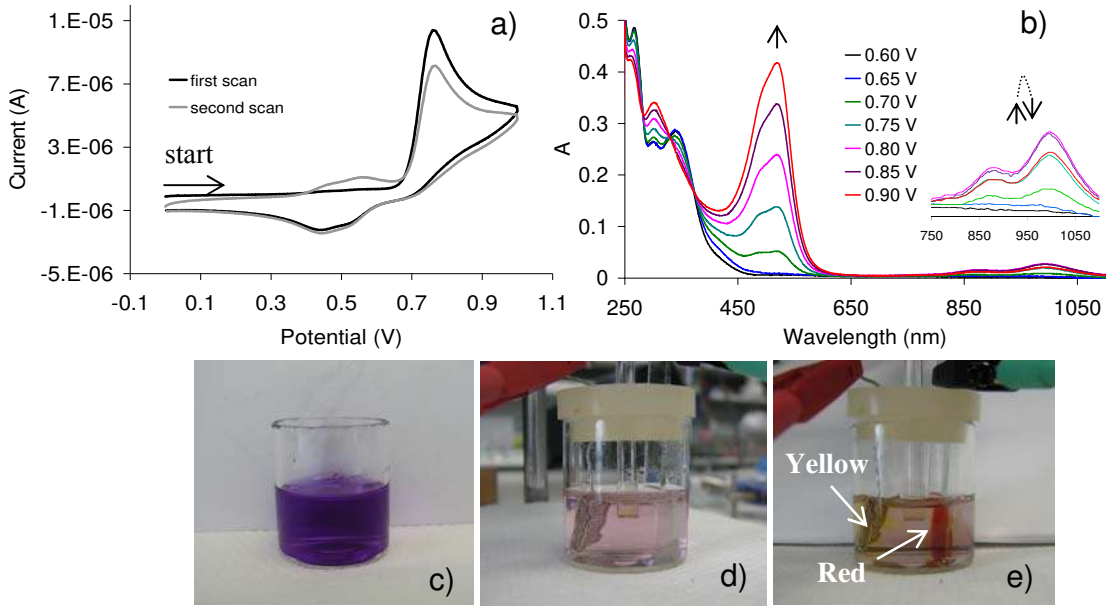

Figure 3. Cyclic voltammograms of **SP1** (a), spectroelectrochemistry during oxidation of $2 \cdot 10^{-3}$ M **SP1** in OTTLE cell (b), a solution of **SP1** just after preparation (c) and after 20 minutes exposure to visible light, (d) change in **SP1** solution in electrochemical cell during applied potential 1 V to the ITO electrode (e). **SP1** concentrations on a) c) d) e) are $1 \cdot 10^{-3}$ M and in acetonitrile with 0.1 M TBAP as electrolyte.

When the **SP1** solution is initially prepared, an equilibrium mixture of the pale yellow **SP1** and red **MC1** forms are clearly present as indicated by the violet coloration (Figure 3c). On standing in the presence of light, this initial equilibrium changes significantly in favor of the **SP1** form, giving the pink colour (Figure 3d). Therefore, oxidation at the working electrode is clearly driving the **SP1** to the **MC1** form (red colour). Zhi et al. proposed a mechanism for this type of electroisomerization.[27] However, they suggested that the isomerization arises from the reduced spiropyran, which can not be the case here. As suggested by Preigh and co-workers for an hydroxyl analogue,[4] initial oxidation of the indoline nitrogen to give the $\mathbf{SP_{ox}}$, followed by rearrangement, affords the **MC** radical cation. During the second scan of the CV of **SP1** (Figure 3a), two new broad overlapping oxidation waves appeared with potential maxima at 0.47 and 0.57 V. Since several stereoisomers of the **MC** form have been recognized,[29] the most dominant of which are the TTC (*trans-trans-cis*) and TTT (*trans-trans-trans*)[30] forms, it is likely that these peaks may represent the electrochemistry of the two **TTC-MC1** and **TTT-MC1** isomers (Scheme 2). These species themselves could undergo reversible electrochemistry as indicated by the

reduction peaks at 0.44 V and 0.52 V. However, there is no apparent electrochemical path back to **SP1** from either the oxidised or reduced **MC1** isomers as is indicated by a drop in height of the **SP1** oxidation peak at 0.77 V on the second scan of the CV (Figure 3a).

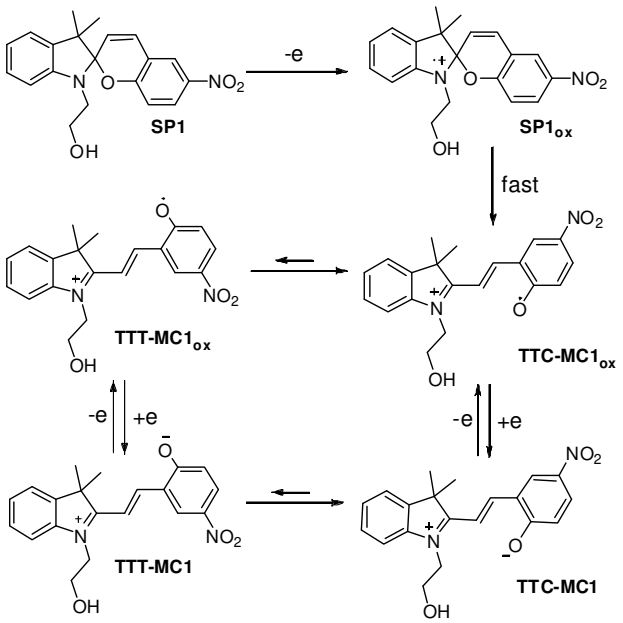

Scheme 2. Postulated mechanism for the electrochemical redox behaviour of **SP1**.

In order to further probe this, the absorption spectral changes of **SP1** oxidation processes in 0.1M TBAP in acetronitrile were recorded at applied potentials from 0.6 to 0.9 V, and are shown in Figure 3b. Significant absorbance changes were observed when the potential exceeded 0.65 V and new absorption bands with maxima at 492 nm and 523 nm (corresponding to the red solution in Figure 3e) grew rapidly. Therefore, we ascribe these two absorption bands to **TTC-MC1$_{ox}$** and **TTT-MC1$_{ox}$**. It is also interesting to note the appearance of two absorption peaks at 880 nm and 997 nm, which rise (0.8 V maximum) and fall as the oxidation potential is increased. These observations provide significant insights into the electrochemistry and spectroelectrochemistry of **poly-TThSP1**, as we discuss later.

Consequently, we propose that electrochemical oxidation of **SP1** irreversibly leads to isomers of oxidised **MC1**, which themselves undergo reversible electrochemistry as depicted in Scheme 2. Although these are solution-based processes, we anticipated that the spiropyran substituent of **poly-TThSP1** would undergo similar electrochemistry given we had not observed any spectroscopic interaction between the terthiophene and spiropyran groups.

3.2. Electrochemical polymerization of TThSP1. The electrochemical deposition of **TThSP1** on a platinum disc electrode shows cyclic voltammograms (CVs) with an increase in current with successive cycles, indicative of successful electroactive film deposition (Scheme 1 and Figure 4a). The electropolymerization process is carried out up to 0.8 V, with the onset of monomer oxidation to its radical cation at 0.62 V (Inset, Figure 4a) and the formation of bluish film, typical of oxidized polythiophene. We do not observe the characteristic red colour of merocyanine at the maximum applied potential of 0.8 V, leading us to conclude, that we do not open the spiropyran ring during electrodepostition. The film-coated electrode was placed in monomer-free solution for post-polymerization CV analysis. The post CVs show interesting, dynamic redox behaviour (Figure 4b). During the first scan in the post CV of **poly-TThSP1**, three oxidation peaks are visible at 0.12, 0.34 and at 0.76 V (Figure 4b). While the origin of the peak at 0.12 V is not clear, the 0.34 V peak can be assigned to oxidation of the polymer backbone (**poly-TTh$_{ox}$SP1**, Scheme 3), since cycling of the **poly-TThSP1** film between -0.4 and 0.5 V shows consistent capacitive behaviour over more than 10 cycles (not shown). A similar oxidation peak is observed for a **poly-TThMA** film (Figure 4c), which is the analogous spiropyran free polymer, with a methyl substituent instead of the nitrobenzospiropyran. In contrast, the sharp oxidation peak at 0.76 V on the first post CV scan of **poly-TThSP1** (Figure 4b) is completely lost during the second scan, but appears to recover somewhat during cycling. The position of this peak is at the same potential as the first oxidation of the **SP1** molecule (Figure 3a). It is likely that the oxidation peak at 0.76 V for **poly-TThSP1** results from loss of an electron from the indoline nitrogen of the **SP1** substituent, leading to the oxidized **MC1** substituent on the oxidized polythiophene backbone (**poly-TTh$_{ox}$MC1$_{ox}$**, Scheme 3).

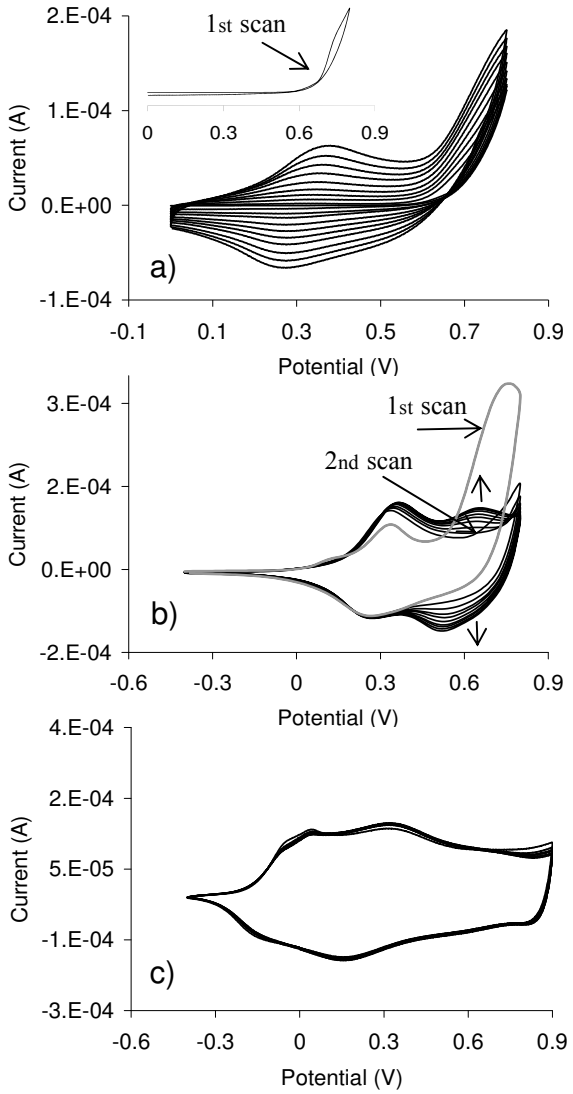

Figure 4. Electrochemical deposition of **TThSP1,** inset shows the first scan (a), post CV voltammogram of **polyTThSP1** (b) and **poly-TThMA** (c) on platinum disc electrode, 10 scans at a scan rate 100 $mV \cdot s^{-1}$.

We also observed that the choice of the switching potential used during electropolymerization of **polyTTh-SP1** (Figure S1a,c,e) influences the electrochemical characteristics of the post CV voltammogram (Figure S1b,d,f). When the switching potential of electropolymerization is set higher than 0.9 V (Figure S1e), somewhat higher than the oxidation potential of spiropyran **SP1 (**0.77 V, Figure 3a), the sharp oxidation peak at 0.76 V on the first post CV scan of **poly-TThSP1** is no longer observed. Clearly, from these post CVs, the oxidation of the appended spiropyran is not reversible, and therefore

it appears likely that the substituent on **poly-TThSP1** remains in the **MC** form following further cycling. The CV following initial **poly-TThSP1** oxidation (2nd scan, Figure 4b) has no peak due to **SP** oxidation but subsequent scans exhibit a peak at 0.65 V of increasing intensity. This could arise from the oxidation of the polymer **MC** stereoisomers, analogous to that postulated for **SP1** (Scheme 2).

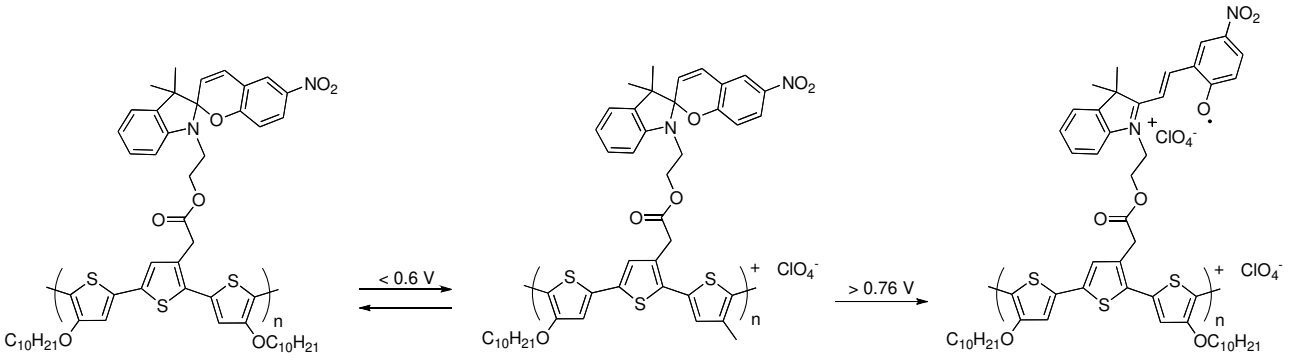

Scheme 3.

This oxidative electroisomerization of **poly-TThSP1** is also supported by the dramatic colour changes observed on oxidation of the polymer film. Polythiophene films generally exhibit two colours, depending on the doped state. For example, the colour of the parent poly(terthiophene) in the reduced state is orange-red and brown-black when the polymer is oxidized.[31] Reduced **poly-TThSP1** film is a violet-pink colour, but on oxidation to 0.5 V (polymer backbone oxidation) the colour changes to green-blue (Scheme 3). Further oxidation to 0.8 V generates a more intense violet-pink film as the result of the formation of the oxidized **MC** substituent. This additional colour change at the positive potential occurs very quickly, over a narrow range of potentials (see movie, Supplementary Information). This unique photochromic behaviour in the doped state was further investigated using spectroelectrochemistry.

3.3. UV-visible spectroelectrochemistry of poly-TThSP1. The spectral properties of **poly-TThSP1** were examined across the potential range used for the post-CV analyses (-0.35 – 0.9 V). **Poly-TThSP1** exhibited typical polythiophene behaviour as the electrode potential was increased from -0.35 to 0.6 V,

with initial polaron band formation (870 nm) followed by the development of a free carrier tail (Figure 5a). As the applied potential increases from 0.6 V, the growth of a new absorbance at 540 nm is observed (Figure 5b), which corresponds to the initial sharp oxidation shown in the post CVs (Figure 4b). This absorbance is in a similar position to that observed for the photoisomerized **TThMC1** monomer (Figure 2, violet line) and therefore we attribute it to the oxidized **MC** isomer of **poly-TTh$_{ox}$MC1$_{ox}$**.

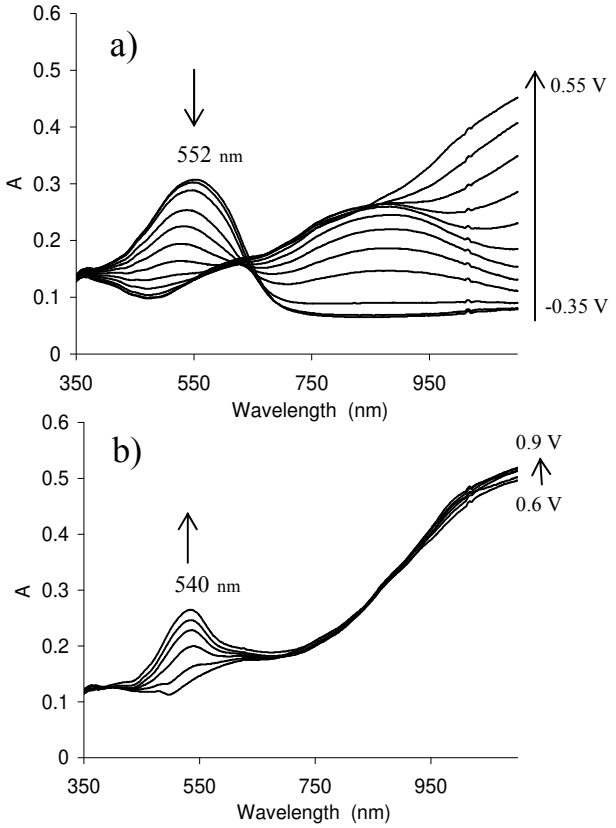

Figure 5. Spectroelectrochemistry of electrochemically polymerized film of **poly-TThSP1** (a and b) on ITO glass for potential ranges of -0.35 – 0.55 V (a) and 0.6 – 0.9 V (b).

In order to probe the reversibility of this merocyanine formation and oxidation, we monitored the 540 nm absorbance over the potential range -0.1 V to 0.9 V during cyclic voltammetry (Figure 6). A freshly electrodeposited film was utilized in order to ensure that the polymer was in the **SP** form. In addition, the same experiment was carried out with a freshly prepared **poly-TThMA**. As seen in the Figure 5a, the absorbance at the potential -0.1 V results from the polymer backbone and, as the polymer becomes oxidized, the absorbance decreases (Figure 6a, black line). When the potential applied to the **poly-**

TThSP1 film is more positive than 0.6 V, the absorbance at 540 nm increases rapidly as a result of **MC** isomer formation. In contrast, **poly-TThMA** film (Figure 6a, grey line) does not show any absorbance changes at the positive potential range, as is expected for a poly(thiophene).

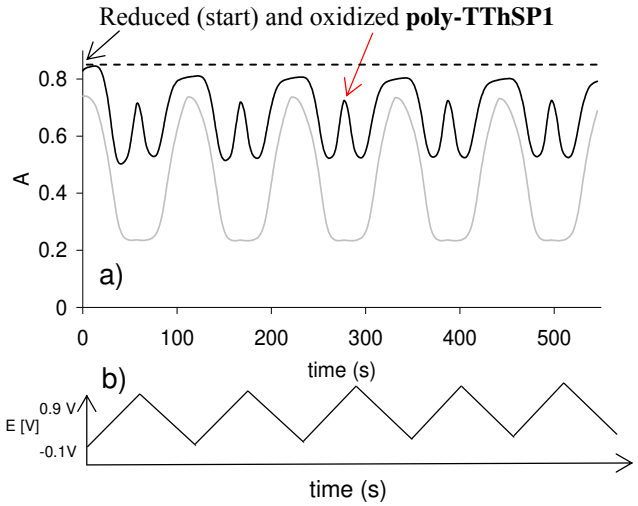

Figure 6. Absorption spectra response at 540 nm for a) **poly-TThSP1** (black line) and **poly-TThMA** (grey line), when the applied potential was changed from -0.1 V to 0.9 V in 0.1 M TBAP in acetonitrile (b).

We also observed following **poly-TThSP1** oxidation for the first time (t = 0, Figure 6a), the same level of absorbance on re-reduction (dashed line, Figure 6a), indicative of the formation of ring opened merocyanine isomers that do not ring close to spiropyran on reduction. This observation is consistent with the variable electrochemical response of **poly-TThSP1** (Figure 4a).

In order to better understand these changes, a spectroelectrochemical study of fresh films of both **poly-TThSP1** (Figure 7) and control sample **poly-TThMA** (see Supporting Information, Figure S2) was undertaken. The aim of these measurements was to monitor the absorbance changes during a "simulation" of the film cycling. The absorbance spectra in the previous spectroelectrochemical study (Figure 5) only show the initial changes that occur following the oxidation of the spiropyran moiety. In this study, absorbance spectra were obtained while holding the potential at: –0.1 V, 0.6 V, 0.8 V and 1.0 V (Figure 7a,b,c,d), potentials at which new peaks appeared in the post-CVs during film cycling (Figure 4b and c). This was repeated six times, effectively mimicking six CV cycles.

Again, it is clear that the spectra recorded during the first "cycle" are different from all the others. Thus, the 1st spectrum of the reduced **poly-TThSP1** film (Figure 7a) is different across the whole spectrum from the next five spectra recorded at that potential (-0.1 V), consistent with the single wavelength observation evident in Figure 6a. As expected up to 0.6 V, the polythiophene backbone appears to be oxidized, as evidenced by the complete loss of the absorbance at 500 nm as well as the rise of the polaron band at 850 nm (Figure 7b). However, the "2nd cycle" shows the rise of a new band below 500 nm, which appears to come from the opening of the spiropyran.

The picture becomes clearer from the absorbance spectra at 0.8 V (Figure 7c) and 1.0 V (Figure 7d). The 1st spectrum at 0.8 V is again assigned essentially to the oxidized polymer backbone, which now shows a significant free carrier tail above 700 nm. The 2nd and later spectra exhibit much more character with two new peaks at 443 and 477 nm and broad absorbances at 870 and 995 nm. All of these bands are then either lost completely or reduce substantially at higher oxidation potential (1.0 V, Figure 7d), with the appearance of a new band around 540 nm and the retention of the free carrier tail.

Therefore, the two bands at 443 and 477 nm are clearly not due to the fully oxidized polymer with oxidized merocyanine, which absorbs at 540 nm. A clue to the origin of these bands lies in the simultaneous appearance of the broad near-infrared absorbances that are almost identical to those observed in the spectroelectrochemistry of the oxidized parent spiropyran **SP1** (Figure 3b). All of these bands appear to arise from the **SP** substituent since an identical spectroelectrochemical experiment involving **poly-TThMA** (see Supporting Information, Figure S2) does not show peaks at 443 and 477 and at 870 and 995 nm following initial polymer oxidation. Since the merocyanin groups are fixed in space by the polymer backbone, the formation of large aggregates is unlikely. However, interaction of two merocyanines with antiparallel dipoles could arise from merocyanines on neighboring polymer chains forming π-dimers. The two peaks at 443 and 477 nm (Figure 7c) could represent dimers formed from the two major merocyanine isomers TTC and TTT (see Scheme 2).

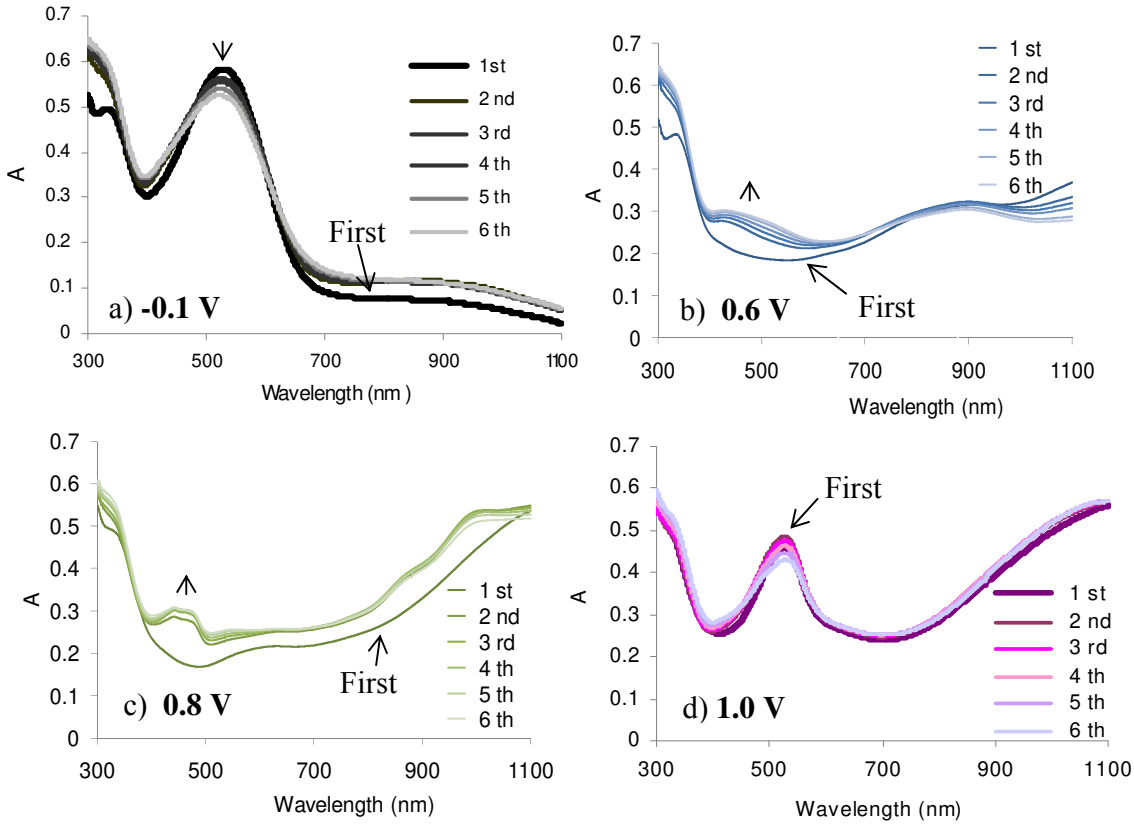

Figure 7. Spectroelectrochemistry of **poly-TThSP1** on ITO recorded six times at the potentials: -0.1 V (a), 0.6 V (b), 0.8 V (c), 1.0 V (d).

The removal of a single electron from this type of π-dimer to form a π-radical cation dimer might then be expected to be easier than oxidation of a single merocyanine substituent. The formation of π-radical cation dimers in aromatic species is well established in the literature.[22,32,33] Both the spectroelectrochemistry of **SP1** solutions (Figure 3b) and that of the **poly-TThSP1** film (0.8 V, Figure 7c) are fully consistent with the formation of merocyanine π-radical cation dimers. In both cases the oxidation of the merocyanine moiety leads to low intensity, longer wavelength peaks between 800 nm and 1100 nm, that rise and fall as the intensity of the oxidized merocyanine band around 500 nm increases. This can be accounted for the initial formation of π-radical cation dimmers at a low concentration of oxidized merocyanine followed by disappearance of the dimmer with complete oxidation of the merocyanine.

The presence of neutral or charged dimeric species or even larger aggregates as a result of merocyanine formation and oxidation accounts for the majority of changes seen in the spectroelectrochemical experiments. In order to clarify this, we have depicted the processes occurring during the first and subsequent electrochemical cycles in cartoon fashion in Scheme 4.

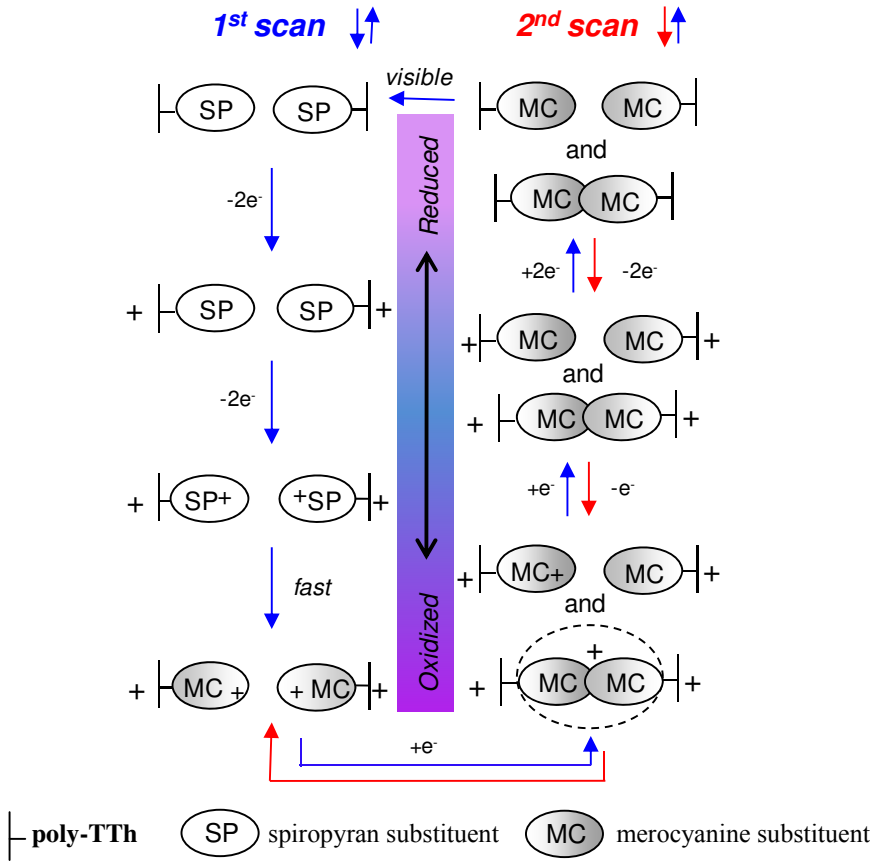

Scheme 4. Cartoon representation of redox cycling and aggregation of **poly-TThSP1**.

The left hand side of the scheme represents the oxidation component of the first cycle with initial polymer oxidation, followed by formation of oxidized spiropyran that rapidly ring opens above 0.8 V to oxidized merocyanine. The reduction component of the first cycle (going up the right hand side of Scheme 4) leads ultimately to a neutral merocyanine-substituted polythiophene that contains both single, as well as dimeric (or oligomeric), merocyanines. This accounts for the loss of peak height and the peak broadening in the second and subsequent spectra of the spectrochemical study at -0.1 V (Figure 7a). As the polymer is oxidized and reduced, more ordering of the film occurs as a result of

strong π-radical cation dimer coupling, leading to an overall increase in neutral dimer formation (and hence peak broadening due to increasing absorptions around 446 nm). This also may explain the apparent increased difficulty in reducing the polymer after the first cycle as evidenced by the increased polaron band at 850 nm.

On the second cycle, it is now the presence of merocyanine π-dimers that dominate the electrochemistry (down the right hand side of Scheme 4). Oxidation of the merocyanine polymer at 0.6 V (Figure 7b) leads to the loss of the neutral polythiophene absorption at 552 nm, revealing broad absorptions from 400 to 550 nm that reflect the presence in the oxidized polymer film of both free merocyanine substituents, as well as merocyanine π-dimers and possibly higher oligomers. Further oxidation (0.8 V, Figure 7c) now gives the characteristic bands of both π-dimers and π-radical cation dimers as well as both oxidized (~540 nm) and neutral merocyanines (~560 nm) on the oxidized polymer backbone. Finally, full oxidation of the merocyanine groups above 1.0 V (Figure 7d) leads to separation of the merocyanines with only the oxidized merocyanine band at 540 nm apparent in the spectrum.

Given that the spiropyran cannot be regenerated electrochemically, we investigated the feasibility of photochemical control of this process in order to achieve complete reversibility of this intriguing redox system.

3.4. Light control of SP1 isomerization. The photochemical conversion of merocyanine to spiropyran is typically an easily identifiable process, as we observed in the study of **SP1**, since the merocyanine absorption spectrum is largely well separated from the spiropyran spectrum. However, in the case of **poly-TThMC1**, the merocyanine absorption (assumed to be around 560 nm as for **TThSP1**) is at similar wavelengths to that of the reduced polyterthiophene backbone (380-670 nm) making identification of merocyanine formation difficult, since absorption of the reduced polymer backbone will compete with merocyanine absorption. In order to ensure the presence of spiropyran in the

polymer, thin films (< 1μm) of **poly-TThSP1** on ITO glass were CV electrodeposited between 0 V and 0.75 V (see Figure S1a), and its UV-visible spectra recorded (Figure 8, blue line), following washing to ensure the absence of excess monomer from the polymerization. Irradiation of the dried film with ultraviolet (UV) light (254 nm, 5 min) afforded a more intense and broad UV-visible band (Figure 8, red line) shifted by 20 nm. This is consisted with formation of **poly-TThMC1**, since the intensity of the polythiophene backbone would be expected to remain constant with growth of a new, broad absorption centered around 560 nm. A small broad absorption at 383 nm also appears. Subsequent irradiation of the polymer film with visible light (40 min) gave a polymer absorption band (Figure 8, green line) identical to that of **poly-TThSP1** albeit with a slightly higher intensity. A second UV light illumination returned the higher wavelength absorption (Figure 8, violet line), again with small intensity differences. The intensity changes may well result from the conformation changes to the polymer backbone as a result of the spiropyran to merocyanine isomerization.

In order to ensure, these spectra changes largely resulted from spiropyran to merocyanine isomerization, irradiation of the control polymer **poly-TThMA** was investigated. No change in the absorption spectra of **poly-TThMA** was observed (see Supporting Information, Figure S3) following exposure of polymer film to UV light. While these experiments demonstrates that reduced **poly-TThSP1** film undergoes the typical reversible **SP** to **MC** isomerization, further experiments were undertaken in order to determine whatever this was the case for the oxidized **poly-TThSP1** film.

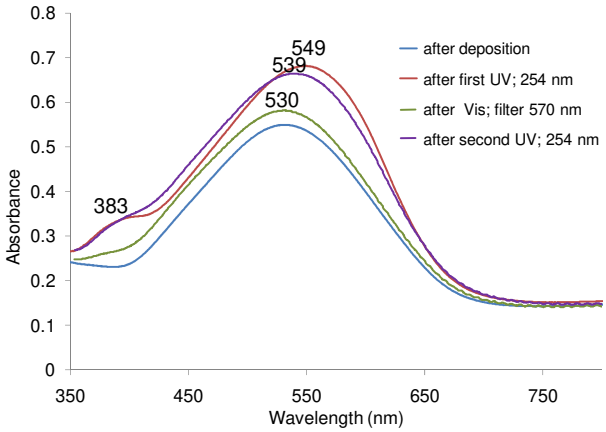

Figure 8. UV-vis spectra of: reduced **poly-TThSP1** after electrochemical deposition (blue line), after first irradiation with 254 nm UV light (red line), followed by irradiation with visible light (green line), and second irradiation with 254 nm UV light (violet line).

TTh-SP1 was electrochemically polymerized on optically transparent ITO-coated glass by chronoamperometric deposition at constant potential (0.8V) in the dark. The **poly-TThSP1** film was exposed to UV light at 254 nm for 5 minutes, and the the post-CVs (from -0.4 to 0.9 V) obtained with the UV light still applied to the polymer film (Figure S4a). No initial electrochemical response ascribed to the spiropyran moiety, as had been previously seen, is observed, suggesting that under these conditions the spiropyran is all converted to merocyanine, giving **poly-TThMC1**. The polymer film was then irradiated with visible light (390-750 nm) for 5 minutes and the CVs again recorded over the same potential range while maintaining the visible light irradiation (Figure S4b). Clearly, there is a photochemical regeneration of spiropyran in the film, as evidenced by the appearance of a new peak at 0.55 V in the first CV scan, and its subsequent loss in the second scan. However, the amplitude of the peak is low, suggesting that only a fraction of the merocyanine substituents in the film are isomerized. Given that the **poly-TThMC1** film will be composed of both free and aggregated merocyanine substituens, spiropyran formation is likely to be sterically limited. In addition, the isomerization must be slow, certainly slower than the time frame of the cyclic voltammetry, since almost no spiropyran is reformed during the subsequent CV scans. This is perhaps not surprising since the reduced merocyanine film, would be much more compact than that of the reduced spiropyran film particularly

with increased formation of π-dimers, making it sterically and energetically more difficult to reform spiropyran.

3.5. Physical properties of poly-TThSP1. It is well known that conducting polymers display actuation behaviour under an external redox potential, due to the movement of counter ions and associated solvent molecules into and out of the polymer, which results in swelling and contraction.[34] According to our earlier spectroelectrochemical study, the initial oxidation of the spiropyran moiety provides some merocyanine dimer or oligomer aggregates within the polymer film. These processes should markedly affect the morphology of **poly-TThSP1**, and for this reason scanning electron micrograph (SEM) analysis of the different redox stages of the polymer was undertaken. SEM images were obtained for four **poly-TThSP1** samples electropolymerized in the same way but then subjected to different redox conditions. Three of those samples were oxidized or reduced at constant potential for 2 minutes. The first image in Figure 9a shows the morphology of the fresh film, obtained after 1 minute constant potential deposition at 0.8 V. The second polymer sample was oxidized at 0.5 V (Figure 9b) from which we expect only polymer backbone oxidation, while the third one was further oxidized to 0.85 V (Figure 9c), leading to oxidation of the spiropyran substituent on the polymer backbone. The last sample was reduced with the potential -0.4V (Figure 9d). The morphology of the fresh **poly-TThSP1** (Figure 9a), shows a globular structure, with features approximately 1 μm in diameter present on the polymer surface. Since the polymer backbone is oxidized with associated perchlorate anions and the bulky spiropyran is still present, this film would be expected to show the most expanded morphology. The film oxidized state at 0.5 V (Figure 9b) showed a similar morphology with fewer of the island-particles present on the surface. This would be consistent with the loss of some of the spiropyran groups following the initial film preparation. Significantly, further oxidation of the polymer to 0.85 V (Figure 9c) gave a film with an entirely different morphology with a distinctive webbed and close-packed structure, consistent with the formation of the at least partially oxidized planar merocyanine.

AFM images confirm the major change in polymer structure that occurs when the **poly-TThSP1** film is oxidized (Figure S5), since the calculated surface roughness of the reduced (root mean squared, rms=181 ± 8.4 nm) and oxidized (127 ± 5.1 nm) **poly-TThSP1** suggest a more porous surface for the reduced polymer, as would be expected for the more bulky **SP** substituent.

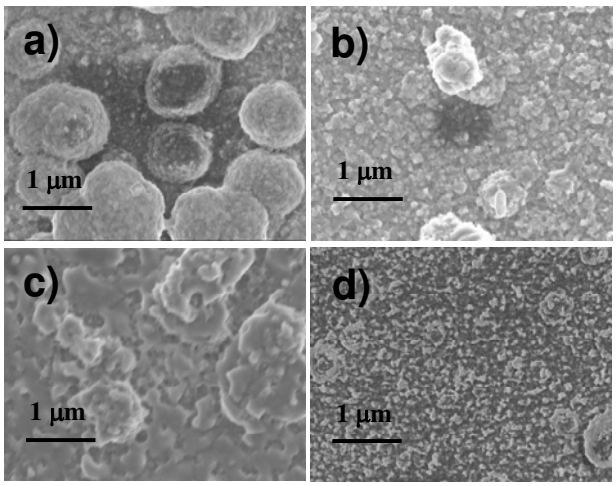

Figure 9. SEM images of **poly-TThSP1** after a constant potential deposition 0.8 V (a), oxidation at 0.5 V (b), oxidation 0.85 V (c), reduction -0.4 V (d).

In order to measure the conductivity, a free standing film of **poly-TThSP1** was obtained after chronoamperometric deposition on ITO-coated glass at a constant potential of 0.8 V for 1 hour and removal from the electrode. A conductivity of 0.4 S cm^{-1} was obtained, the same order of magnitude as that reported by Gallazzi et al. for an analogous poly(alkoxyterthiophene) substituted with the somewhat smaller electron-withdrawing dicyanoethenyl group.[35]

4. Conclusion

The integration of the photochromic properties of spiropyrans with the electrical and optical properties of polythiophenes presents exciting opportunities for a variety of applications. This inspired us to successfully electropolymerize, for the first time, a terthiophene monomer modified with a nitrospiropyran substituent. The resulting polymer, **poly-TThSP1**, displayed a number of different

coloured states on electrochemical redox cycling with associated complex electrochemistry. In order to understand this, we undertook a detailed electrochemical study of the nitrospiropyran precursor **SP1** since little had been reported in the extensive spiropyran literature. We have shown that **SP1** initially undergoes irreversible electrooxidative ring opening to give at least two oxidized merocyanine isomers, which can further undergo reversible redox processes. This behaviour is reflected in the electrochemical processes observed for **poly-TThSP1**. The polymer is initially formed with the spiropyran intact and can undergo typical polythiophene redox cycling at potentials below 0.6 V. However, oxidation of the polymer film above 0.8 V leads to spiropyran oxidation and irreversible isomerization to the oxidized merocyanine. A detailed spectroelectrochemical study of the resulting reduction and further redox cycling revealed that the electrochemical and physical properties of the polymer are then dominated by the presence of the merocyanine and its ability to form π-dimers or oligomers and π-radical cation dimers. The photochemical behaviour of **poly-TThSP1** is dramatically influenced by the electrochemistry. Typical **SP** to **MC** isomerization within the polymer film occurs only if the polymer film has been exposed to oxidation potentials (below 0.8 V). Once the merocyanine is oxidized, the photochemical behaviour of the film is limited. Therefore, the redox properties of **poly-TThSP1** can be used to control its photochemical behaviour. As expected given the large conformational differences between spiropyrans and merocyanines, there are significant morphological changes in the polymer film, although the polymer conductivity does not appear to be dramatically affected and is similar to that of previous polythiophenes.

This unique multichromophoric and multiswitchable polymer system provides an exciting platform for the development of future materials that can exploit the other physical and chemical properties of spiropyrans and merocyanins such as variation in hydrophobicity, ion and molecular complexation and conformational effect leading to polymer actuation. Studies to this end are underway in our laboratories.

Acknowledgment. Financial support from the Australian Research Council and funding from Science Foundation Ireland under award 07/CE/I1147 "CLARITY: Centre for Sensor Web Technologies" is gratefully acknowledged.

Supporting Information Available. The synthesis of methyl 4,4′′-didecyloxy-2,2′:5′,2′′-terthiophene-3′-acetate (**TThMA**), 4,4′′-didecyloxy-2,2′ :5′,2′′-terthiophene-3′-acetic acid (**TThAA**), 2-(3,3′′-dimethylindoline-6′-nitrobenzospiropyranyl)ethyl 4, 4′′-didecyloxy-2, 2′ :5′, 2′′-terthiophene-3′-acetate (**TThSP1**), electrochemical polymerization of **TThSP1** and **TThMA**, UV-vis spectroelectrochemistry, SEM and AFM imaging details and AFM images, conductivity measurements and a movie file showing the colour changes associated with the CV scan of **poly-TThSP1**. This material is available free of charge via the Internet at http://pubs.acs.org.

References

(1) Browne, W. R.; Feringa, B. L. *Annual Review of Physical Chemistry* **2009**, *60*, 407-428.

(2) Fischer, E.; Hirshberg, Y. *Journal of the Chemical Society* **1952**, 4522-4524.

(3) Duerr, H.; Bouas-Laurent, H.; Editors *Studies in Organic Chemistry 40: Photochromism: Molecules and Systems*, **1990.**

(4) Preigh, M. J.; Stauffer, M. T.; Lin, F.-T.; Weber, S. G. *Journal of the Chemical Society, Faraday Transactions* **1996**, *92*, 3991-3996.

(5) Berkovic, G.; Krongauz, V.; Weiss, V. *Chemical Review* **2000**, *100*, 1741-1753.

(6) Willner, I.; Willner, B. *Journal of Materials Chemistry* **1998**, *8*, 2543-2556.

(7) Willner, I.; Willner, B. *Bioelectrochemistry and Bioenergetics* **1997**, *42*, 43-57.

(8) Scarmagnani, S.; Walsh, Z.; Slater, C.; Alhashimy, N.; Paull, B.; Macka, M.; Diamond, D. *Journal of Materials Chemistry* **2008**, *18*, 5063-5071.

(9) Katsonis, N.; Lubomska, M.; Pollard, M. M.; Feringa, B. L.; Rudolf, P. *Progress in Surface Science* **2007**, *82*, 407-434.

(10) Seki, T.; Ichimura, K. *Macromolecules* **1990**, *23*, 31-5.

(11) Byrne, R. J.; Stitzel, S. E.; Diamond, D. *Journal of Materials Chemistry* **2006**, *16*, 1332-1337.

(12) Lee, J.; Kwon, T.; Kim, E. *Tetrahedron Letters* **2006**, *48*, 249-254.

(13) Wesenhagen, P.; Areephong, J.; Fernandez Landaluce, T.; Heureux, N.; Katsonis, N.; Hjelm, J.; Rudolf, P.; Browne, W. R.; Feringa, B. L. *Langmuir* **2008**, *24*, 6334-6342.

(14) Hugel, T.; Holland Nolan, B.; Cattani, A.; Moroder, L.; Seitz, M.; Gaub Hermann, E. *Science* **2002**, *296*, 1103-1106.

(15) Ustamehmetoglu, B. *Polymers for Advanced Technologies* **1999**, *10*, 164-168.

(16) Roncali, J. *Chemical Reviews* **1992**, *92*, 711-38.

(17) Li, Y.; Zou, Y. *Advanced Materials* **2008**, *20*, 2952-2958.

(18) Ahn, S.-H.; Czae, M.-z.; Kim, E.-R.; Lee, H.; Han, S.-H.; Noh, J.; Hara, M. *Macromolecules* **2001**, *34*, 2522-2527.

(19) Areephong, J.; Kudernac, T.; de Jong, J. J. D.; Carroll, G. T.; Pantorott, D.; Hjelm, J.; Browne, W. R.; Feringa, B. L. *Journal of the American Chemical Society* **2008**, *130*, 12850-12851.

(20) Park, I. S.; Jung, Y.-S.; Lee, K.-J.; Kim, J.-M. *Chemical Communications 46*, 2859-2861.

(21) Gallazzi, M. C.; Castellani, L.; Marin, R. A.; Zerbi, G. *Journal of Polymer Science, Part A: Polymer Chemistry* **1993**, *31*, 3339-3349.

(22) Grant, D. K.; Jolley, K. W.; Officer, D. L.; Gordon, K. C.; Clarke, T. M. *Organic & Biomolecular Chemistry* **2005**, *3*, 2008-2015.

(23) Wagner, K.; Crowe, L. L.; Wagner, P.; Gambhir, S.; Partridge, A. C.; Earles, J. C.; Clarke, T. M.; Gordon, K. C.; Officer, D. L. *Macromolecules*, *43*, 3817-3827.

(24) Gambhir, S.; Wagner, K.; Officer, D. L. *Synthetic Metals* **2005**, *154*, 117-120.

(25) McCoy, C. P.; Donnelly, L.; Jones, D. S.; Gorman, S. P. *Tetrahedron Letters* **2007**, *48*, 657-661.

(26) Campredon, M.; Giusti, G.; Guglielmetti, R.; Samat, A.; Gronchi, G.; Alberti, A.; Benaglia, M. *Journal of the Chemical Society, Perkin Transactions 2: Physical Organic Chemistry (1972-1999)* **1993**, 2089-94.

(27) Zhi, J. F.; Baba, R.; Hashimoto, K.; Fujishima, A. *Journal of Photochemistry and Photobiology, A: Chemistry* **1995**, *92*, 91-97.

(28) Jukes, R. T. F.; Bozic, B.; Hartl, F.; Belser, P.; De Cola, L. *Inorganic Chemistry* **2006**, *45*, 8326-8341.

(29) Heiligman-Rim, R.; Hirshberg, Y.; Fischer, E. *Journal of Physical Chemistry* **1962**, *66*, 2465-2470.

(30) Hobley, J.; Malatesta, V. *Physical Chemistry Chemical Physics* **2000**, *2*, 57-59.

(31) Roncali, J.; Garnier, F.; Lemaire, M.; Garreau, R. *Synthetic Metals* **1986**, *15*, 323-331.

(32) Brancato-Buentello, K. E.; Kang, S.-J.; Scheidt, W. R. *Journal of the American Chemical Society* **1997**, *119*, 2839-2846.

(33) van Haare, J. A. E. H.; Groenendaal, L.; Havinga, E. E.; Meijer, E. W.; Janssen, R. A. J. *Synthetic Metals* **1997**, *85*, 1091-1092.

(34) Wallace, G. G.; Spinks, G. M.; Teasdale, P. R.; Editors *Conductive Electroactive Polymers: Intelligent Materials Systems*, **1996**.

(35) Gallazzi, M. C.; Toscano, F.; Paganuzzi, D.; Bertarelli, C.; Farina, A.; Zotti, G. *Macromolecular Chemistry and Physics* **2001**, *202*, 2074-2085.

For Table of Contents use only

A multiswitchable poly(terthiophene) bearing a spiropyran functionality: understanding photo and electrochemical control.

Klaudia Wagner, Robert Byrne, Michele Zanoni, Sanjeev Gambhir, Lynn Dennany, Robert Breukers, Michael Higgins, Pawel Wagner, Dermot Diamond, Gordon G. Wallace and David L. Officer